Fan-Type AMC Surface for Broadband Low-RCS Applications

Xueyan Song [1], Lei Chen [2], Zehong Yan [2], and Yanyan Li [3]

[1] School of Electronic Engineering
Xi'an University of Posts & Telecommunications, Xi'an, 710121, China
xysong6597@126.com

[2] National Key Laboratory of Antennas and Microwave Technology
Xidian University, Xi'an, 710071, China
leichen@mail.xidian.edu.cn, zhyan@mail.xidian.edu.cn

[3] National Key Laboratory of Science and Technology on Aerospace Intelligent Control
Beijing, 100854, China
liyanyan0418@126.com

Abstract ─ An artificial magnetic conductor (AMC) surface is proposed in this paper to reduce radar cross section (RCS) by more than 10 dB in a broad frequency band. The proposed AMC structure consists of two different units - seven hexagonal circles and Jerusalem cross loaded with four L-type branches, contributing to a wide phase difference ($180°\pm37°$) frequency band. To obtain a low RCS value, the two proposed units are arranged in fan-type for the AMC surface. The simulated results show that the RCS can be reduced by more than 10 dB in a broad frequency band from 12.2 to 27 GHz (75.5%). The proposed AMC structure combined by 20×20-unit cells is fabricated and measured in anechoic chamber. Measured results in the band below 18 GHz of the fabricated prototype agree well with the simulated ones, which validates that the proposed AMC surface may be utilized on low-RCS platforms.

Index Terms ─ AMC, broadband, RCS reduction.

I. INTRODUCTION

With the rapid development of stealth and anti-stealth technology, materials for radar cross section (RCS) reduction in wide band have been paid more attention. To reduce RCS, there have been several techniques, such as metamaterial absorbers [1-2], Salisbury screen [3], electromagnetic band gap (EBG) [4-5], etc. Nevertheless, with the structures proposed above, the RCS can only be reduced in narrow frequency bands.

AMCs attract much attention because of their phase characteristics. With in-phase reflection property, AMC can be utilized to obtain low-profile antennas [6-7] and to enhance gain of antennas [8]. Moreover, AMCs play an important role in low-RCS designs. To obtain low-RCS characteristic in broad band, many RCS suppressing metasurfaces [9-15] have been proposed, among which, design of checkerboard configuration combined by AMC structures [10-15] has gradually been a more popular and effective method. In the beginning, a planar chessboard arranged by AMC and PEC is proposed by Paquay in 2007 [10]. With that configuration, the energy can be scattered in other directions after it reaches the surface and a cancellation of energy in boresight direction can be obtained. That is because, the metallic cells can reflect incident waves with a $180°$ change of phase, and AMC units can bring in no phase change at the operation frequency. By arrangement of the two units, destructive interference is produced, and a null can be achieved in normal direction. However, the bandwidth for RCS reduction is limited by the narrow in-phase reflection bandwidth of AMC. To obtain a wider bandwidth for RCS reduction, surfaces arranged by AMC unit cells with different dimensions [11-12] or different structures [13-16] have been presented, resulting in broad phase difference ($180°\pm37°$) bands. In [11], a novel polarization-insensitive metasurface which consists of four inter-twined subarrays, is investigated for ultra-broadband RCS reduction. The unit is a disc-shaped metallic patch with a concentric metallic ring patch. Consists of carefully arranged units with spatially varied dimension, the surface can achieve more than 10 dB RCS reduction in the band from 7 to 12 GHz. In addition, Pei Yao designed a miniaturized chessboard-like AMC reflecting screen [12], which is arranged by two different square AMC unit cells. The in-band RCS reduction is obtained in the band ranging from 13.4 to 20.5 GHz, and the out-of-band RCS reduction is achieved by cancellation between the approximately PEC and AMC in the band of 20.5-26.9 GHz. The measured results

show that the proposed surface can achieve 10 dB RCS reduction in the band from 13.5 to 28.1 GHz (70.2%). Additionally, an AMC structure, consisting of two different types of AMCs, is proposed for ultra-thin and broadband radar absorbing material design in [13]. The measured results show that, the screen achieved a wide phase difference band from 13.25 to 24.2 GHz, in which the RCS is reduced by 10 dB except for some frequency shift. Moreover, a hexagonal checkerboard and a square checkerboard are designed and compared with each other in [14] for wideband RCS reduction. They are composed of two kinds of AMC units utilizing square- and circular- shaped patches and realize over 60% frequency bandwidth for 10 dB RCS reduction. In [15], an AMC surface, combined by two different AMC unit cells, is designed as the ground of a low scattering microstrip antenna. The RCS is reduced by 10 dB in a wide band from 6 to 13.4 GHz and the maximum RCS reduction is 17 dB at 10 GHz. It can be seen that most of the array arrangements of AMC or PEC unit cells in the above references are chessboard. To obtain larger RCS reduction values, a fan type arrangement of AMC unit cells is employed in this paper as proposed in [16] to enhance the cancellation effect by increase the common boundaries of the two units. The low-RCS screen is combined by square loop and square patch units. However, the simulated results show that the bandwidth in [16] remains to be improved.
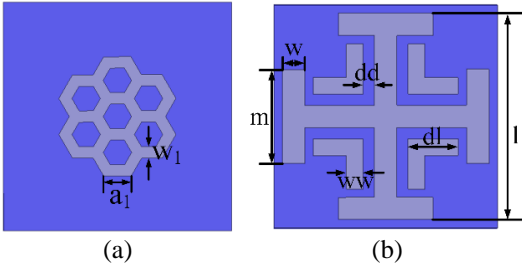

Fig. 1. Unit cells designs for: (a) AMC1 and (b) AMC2.

Based on the previous research in paper [17], an AMC surface for broadband RCS reduction is proposed in this paper to achieve a wider low-RCS bandwidth and a larger RCS reduction value simultaneously. With two new-style AMC unit cells, phase difference $(180°\pm37°)$ of the reflective waves is produced in a broad frequency range, which can contribute to a wide band for 10 dB RCS reduction. To further decrease the RCS value, the fan type arrangement of AMC unit cells is adopted in this paper. A broad band from 12.2 GHz to 27 GHz (75.5%) of 10 dB RCS reduction is obtained. Moreover, the designed AMC surface is fabricated and measured in anechoic chamber. A good agreement between the simulated and measured results shows that the presented AMC surface can be employed for broadband low-RCS

applications.

II. DESIGN AND ANALYSIS OF AMC SURFACE

A. Design principle of broadband AMC surface

From [17, 18], when plan waves radiate normally on the AMC surface, the total energy reflected from the surface equals the total of the reflected energy from all AMC blocks. Assume that the reflection magnitude of all the AMC blocks is equal to A, which keeps no change with frequency. Hence, based on the concept of standard array theory [9, 10], the total reflected field is,

$$E_r = 2Ae^{j\bullet\varphi_1} + 2Ae^{j\bullet\varphi_2} = 2Ae^{j\bullet\varphi_1}(1 + e^{j\bullet(\varphi_2-\varphi_1)}), \quad (1)$$

where, A is the reflection magnitude of the AMC blocks; φ_1 and φ_2 is the reflection phase of AMC1 and AMC2, respectively. It can be seen from (1) that, when $\varphi_2 - \varphi_1 = \pm180°$, the total reflected field is zero. In other words, the reflected energy from the two AMCs can be totally canceled out. However, the reflection phase is a variable which changes with frequency. In general, compared with PEC surface with the equal size, the reflection which can be reduced by more than 10 dB in boresight direction is set as a criterion [17] and it can be express as the following inequality:

$$|E_r|^2 / |E_{pec}|^2 \leq -10dB, \quad (2)$$

where, E_{pec} represents the total reflection field of PEC surface of the same dimension. From the inequality (2) above, it can be calculated the effective reflection phase difference of the presented AMC surface, which is:

$$143° \leq |\varphi_2 - \varphi_1| \leq 217°. \quad (3)$$

Consequently, the phase difference ranging from $143°$ to $217°$ is considered to be effective for subsequent analysis.

B. Design and analysis of AMC surface

To obtain a wide enough phase difference frequency band, the $0°$ phase reflection frequency of one unit should be as close to the $180°$ phase reflection frequency of the other unit as possible. A great many kinds of AMC units have been designed to constitute AMC surfaces, such as square patches, circle patches, Jerusalem Crosses, rings, etc. [11-16]. After an extensive analysis of their frequency behaviors, hexagon rings and Jerusalem Cross in Fig. 1 are designed as the two AMC units. Since it has a first-mode resonant frequency two times that of other ring types with the exception of the square spiral element and its second resonance is approximately three times that of the fundamental one, the hexagonal ring has superior bandwidth characteristic [19]. Therefore, to obtain a broad in-phase reflection bandwidth, the AMC unit cell1 is made up of seven hexagons, which can generate a $0°$ reflection phase at the center frequency of the required operating band and contribute to a gentler phase curve than a unit combined by one single hexagon. The AMC unit cell2 is a Jerusalem Cross loaded with

four L-type branches. The Jerusalem Cross is used to product a 180° reflection phase at the center frequency, and the four L-type branches are loaded to make the reflection phase curves located at the two sides of the 180° phase reflection frequency smoother. The two kinds of metal units are etched on a 2-mm-thickness F4B (ε_r=2.65, tanδ=0.002) substrate, which is loaded with metallic ground plane to achieve total reflection. To obtain a wide bandwidth in the band higher than 12 GHz (λ_L=25 mm), the unit dimension of the proposed AMC should be in the range from 0.1λ_L to 0.2λ_L (2.5 mm~5 mm). In consideration of the complexity of the unit design, the AMC unit dimension is chosen as 4 mm. The optimized parameters of the two AMC units are listed in Table 1.

Table 1: Optimized parameters of the two AMC units

Parameters	Values	Parameters	Values
a1	0.48 mm	w	0.4 mm
w1	0.2 mm	dd	0.2 mm
l	3.7 mm	dl	0.9 mm
m	1.69 mm	ww	0.3 mm

The reflection phase properties of the two AMC unit are calculated by ANSYS HFSS, which utilizes a unit cell with Floquet-port excitation and master/slave boundaries. As can be obtained in Fig. 2 (a), the AMC unit cell1 demonstrates a 0° phase reflection value at 20 GHz. In addition, near the location of the 0° reflection phase frequency point of AMC unit cell1, the AMC unit cell2 depicts a 180° reflection phase at 19 GHz, which contributes to a broad reflection phase difference frequency band. As shown in Fig. 2 (b) is the reflection phase difference curve between the two AMCs. It illustrates that a reflection phase difference (180°±37°) frequency band ranging from 11.6 GHz to 28.1 GHz for normal incidence can be obtained. Consequently, with the two novel types of AMC units, a wide band of 83.1% for 10 dB RCS reduction can be expected compared with the phase difference bandwidth results achieved in [11-15].

Of all the parameters, parameters a_1, l, and dd have a great impact on the reflection phase property of the two AMC units, as can be seen in Figs. 3 (a-c). The values of a_1 and l determine the center frequency of the two AMC unit cells. To make the phase difference in high frequency band be lower than 217° on the basis of wide phase different bandwidth, the values of a_1 is chosen as 0.48 mm. For the compromise of wide phase different bandwidth and the phase difference in low frequency band, which should be lower than 217°, the value of l is decided to be 3.7 mm. In addition, from Fig. 3 (c), it can be obtained that the parameter dd makes an effect on the reflection phase beside the 180° phase reflection frequency of AMC unit cell2, which finally determines

the phase difference between the two AMC units.

(a) Reflection phases
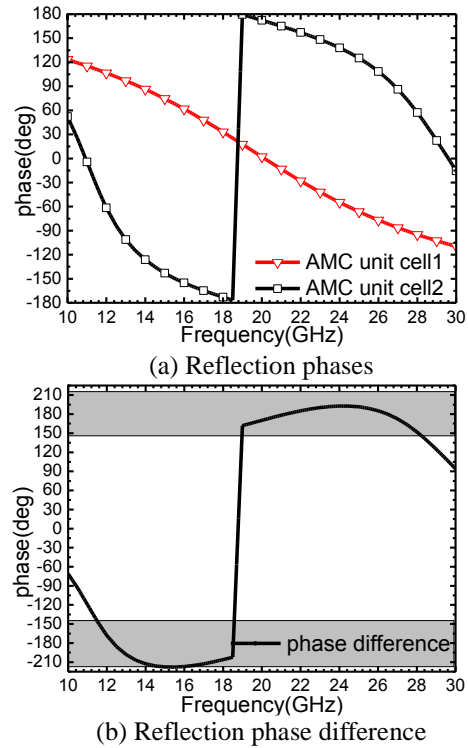

(b) Reflection phase difference

Fig. 2. (a) Reflection phases for both AMCs, and (b) reflection phase difference between two AMCs versus frequency.

Once the dimensions of the two units are fixed, the AMC configuration can be designed. To further decrease the RCS value, the AMC surface is made up of the two units by fan-type arrangement, as shown in Fig. 4. While, an array with an infinite dimension cannot be fabricated in applications. Thus, an array combined by finite number of units need to be designed. If the number of units is too small, the frequency band will move to high frequency and there will be poor property of the phase cancellation between two type of units, which makes it difficult to reduce RCS in the required band. In addition, too large number of AMC units will cause the grating lobes to converge in the edge direction [10], which go also against the RCS reduction. According to the research on AMC structure in [14] and [15], an array arranged by 20×20 units are enough to valid the simulated results in an infinite environment and to be utilized to reduce RCS. Therefore, an AMC surface, the dimensions of which is 80×80 mm², is arranged by 20×20-unit cells in this paper. With fan-type arrangement, the number of interfaces between different units can be increased, which helps the energy be scattered more effectively in non-specular directions [16, 17]. Therefore, the proposed AMC array can obtain a larger value for RCS reduction.
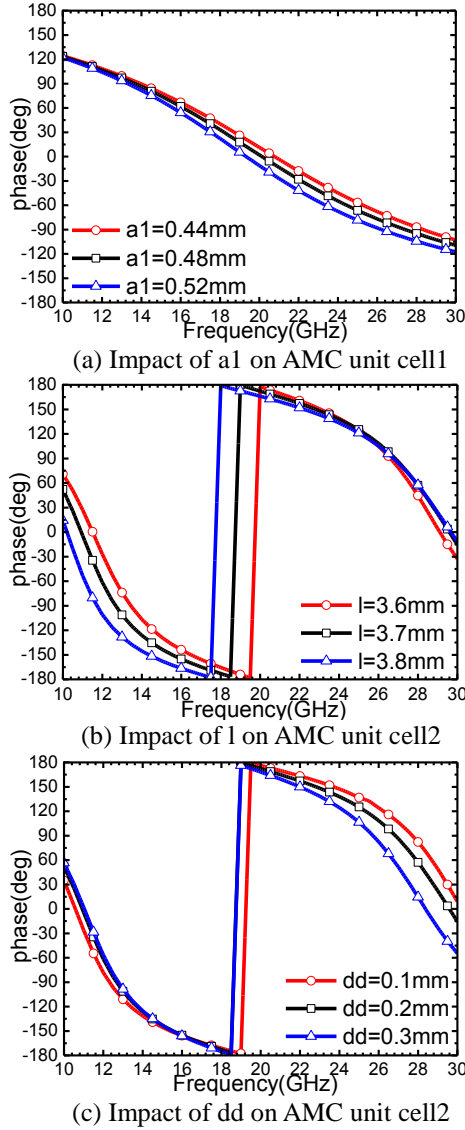
(a) Impact of a1 on AMC unit cell1

(b) Impact of l on AMC unit cell2

(c) Impact of dd on AMC unit cell2

Fig. 3. (a) Impact of a_1 on the reflection phase of AMC unit cell1, and impact of (b) l, and (c) dd on the reflection phase of AMC unit cell2.
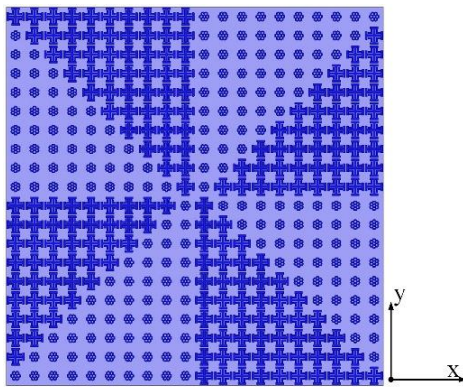

Fig. 4. Top view of the AMC surface configuration.

III. EXPERIMENT AND SIMULATION RESULTS AND DISCUSSION

A. Simulated results

To evaluate the RCS reduction bandwidth of the proposed AMC surface, the monostatic RCS of the AMC surface and PEC surface with equal size for normal incidence is simulated, and Fig. 5 (a) shows the co- and cross-polarized RCS under normal incidence for both x and y polarizations. To calculate the value of RCS reduction, the RCS values are normalized with respect to the PEC surface, as demonstrated in Fig. 5 (b). It can be obtained from the simulated RCS reduction curve, a broad 10 dB RCS reduction frequency band ranging from 12.2 GHz to 27 GHz (75.5%) for x-polarization and from 12.2 GHz to 27.2 GHz (76.1%) for y-polarization is achieved. And the maximum co-polarized RCS reduction, which is more than 30 dB, is obtained at 23 GHz. The simulated RCS reduction band agrees well with the phase difference frequency band (11.6-28.1 GHz) of the two unit cells discussed in the previous section.

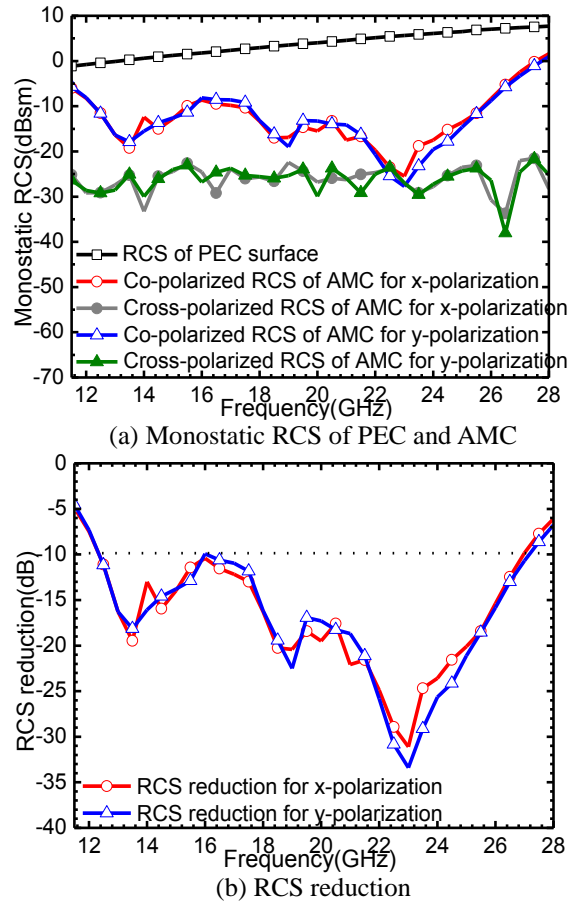(a) Monostatic RCS of PEC and AMC

(b) RCS reduction

Fig. 5. Simulated monostatic RCS of the proposed AMC surface and PEC surface with the equal size and the simulated RCS reduction of the proposed AMC structure under normal x- and y-polarized incident waves.

Moreover, Fig. 6 depicts the normalized bistatic RCS of the proposed AMC surface at 20 GHz (which is close to the center frequency point of the RCS reduction band). It shows that it can be achieved about more than 20 dB RCS reduction at 20 GHz by the proposed AMC surface for x polarization in all incident angles. In addition, Fig. 7 demonstrates the simulated 3-D normalized bistatic RCS for x polarization of the proposed AMC surface and PEC surface with the same dimension at 20 GHz. Compared with the bistatic RCS of PEC surface, the designed AMC surface achieves low RCS in boresight direction and reflects the scattering energy in other directions.
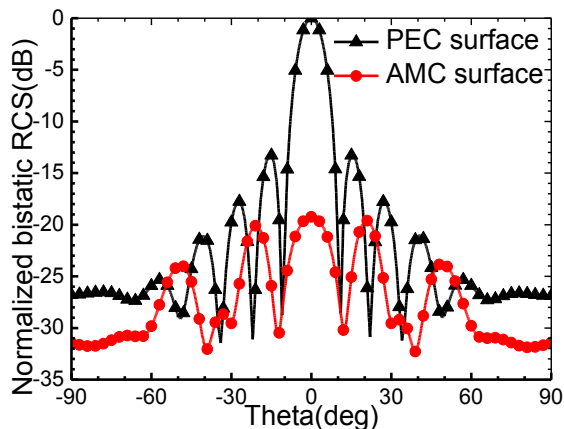

Fig. 6. Simulated 2-D normalized bistatic RCS of the proposed AMC surface and PEC surface for x polarization under normal incidence at 20 GHz.

B. Fabrication and measured results

To validate the simulated RCS property, the proposed AMC surface with dimensions of $80 \times 80 \text{mm}^2$ is fabricated, as shown in Fig. 8 (a), and is measured by the compact antenna test range method in anechoic chamber, as depicted in Fig. 8 (b). Owing to the limit of test factor, the monostatic RCS of the fabrication is measured in the band below 18 GHz.

From the simulated results in Fig. 5, it can be obtained that the co-polarized RCS for y polarization is similar to that for x polarization owing to the approximate rotational symmetry of the AMC structure. Therefore, the co-polarized RCS of the AMC surface for x polarization is measured only. Figure 9 (a) illustrates the measured monostatic RCS of the proposed AMC surface and PEC surface (a replacement by an aluminum sheet) with the same dimension under normal incidence for x polarization. By normalizing with respect to the equal size PEC surface, Fig. 9 (b) demonstrates the measured RCS reduction of the fabricated AMC surface. It can be obtained from the measured results that the RCS

reduction frequency band below 18 GHz ranges from 13.16 to 18 GHz. Compared with the simulated frequency band (12.2-18 GHz), there is a good agreement between the simulated and measured results except for a little frequency shifting, which is caused by fabricated and measured errors and the limited size of the fabricated AMC surface.
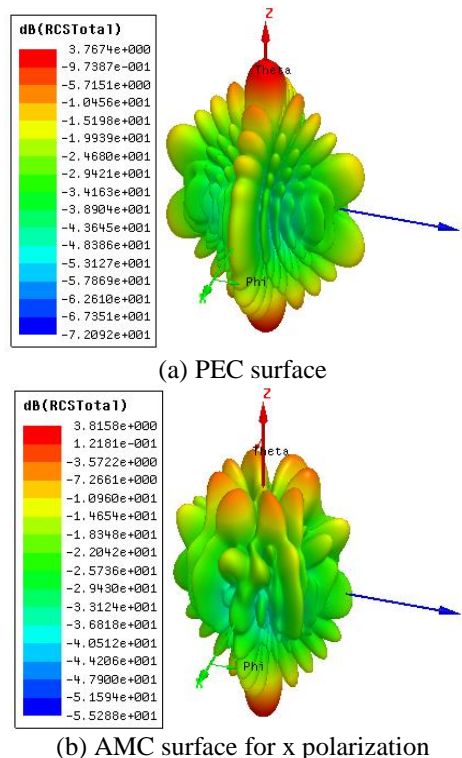

(a) PEC surface

(b) AMC surface for x polarization

Fig. 7. Simulated 3-D normalized bistatic RCS of the proposed AMC surface and PEC surface for x polarization under normal incidence at 20 GHz.

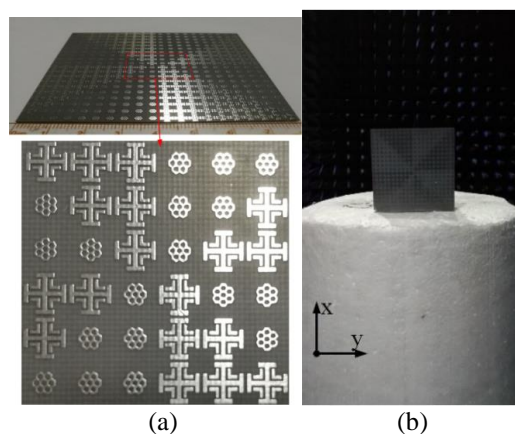(a)   (b)

Fig. 8. Photograph of fabricated fan-type AMC surface and its measured environment.
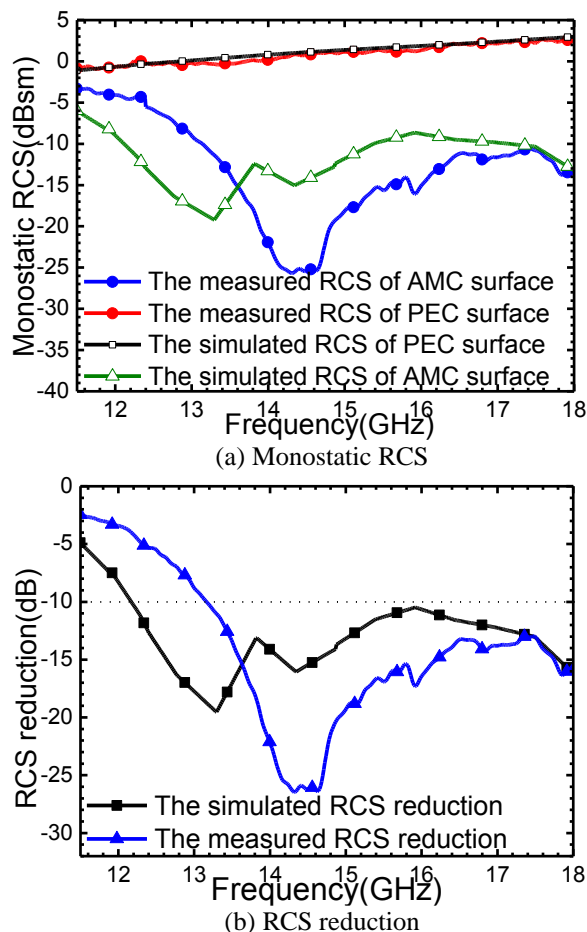
(a) Monostatic RCS

(b) RCS reduction

Fig. 9. Simulated and measured co-polarized: (a) monostatic RCS of the proposed AMC surface and PEC surface with the equal size, and (b) RCS reduction of the proposed AMC surface under normal incidence for x polarization.

Table 2: Comparison on the simulated and measured performances with previously proposed AMC surface

Ref.	Phase Difference BW (GHz)	Simulated 10 dB RCS Reduction BW (GHz)	Measured 10 dB RCS Reduction BW (GHz)
[11]	--	7-12 (52.8%)	7-12 (52.8%)
[12]	12.1-20.5 (51.5%)	13.4-26.9 (67%)	13.5-28.1 (70.2%)
[13]	13.25-24.2 (58.5%)	13.25-24.2 (58.5%)	--
[14]	--	3.76-7.51 (67%)	4.1-7.59 (60%)
[15]	6-14 (80%)	6-13.4 (76%)	6-12 (66.7%)
Our work	11.6-28.1 (83.1%)	12.2-27.2 (76.1%)	13.16- …

Table 2 depicts the comparison performances of the designed AMC structure to the previously proposed AMC surface. From the compared results, it can be demonstrated that the fan-type AMC configuration presented in this paper can achieve wider phase difference frequency band and broader bandwidth for 10 dB RCS reduction.

IV. CONCLUSION

A novel AMC surface is investigated to achieve RCS reduction in a wide band. The configuration is combined by two kinds of unit cells - hexagon rings and Jerusalem crosses. With these two novel units, a reflection phase difference ($180°±37°$) band from 11.6 GHz to 28.1 GHz for normal incidence can be obtained. Furthermore, with a fan type arrangement by the two units, the proposed AMC surface demonstrates a broad 10 dB RCS reduction frequency band ranging from 12.2 GHz to 27 GHz (75.5%) for x-polarization and from 12.2 GHz to 27.2 GHz (76.1%) for y-polarization. Then, the proposed AMC surface with dimensions of $80×80$ mm^2 is fabricated and measured by the compact antenna test range method in anechoic chamber. The agreement between the measured and simulated results in the band below 18 GHz verifies that the proposed AMC configuration can be utilized in low-RCS platforms.

REFERENCES

[1] Y. Ishii, T. Masaki, N. Michishita, H. Morishita, and H. Hada, "RCS reduction characteristics of thin wave absorbers composed of flat and curved metasurfaces," *2016 International Symposium on Antennas and Propagation (ISAP)*, pp. 192-193, 2016.

[2] Z. X. Zhang and J. C. Zhang, "RCS reduction for patch antenna based on metamaterial absorber," *2016 Progress in Electromagnetic Research Symposium (PIERS)*, pp. 364-368, 2016.

[3] K. L. Ford and B. Chambers, "Tunable single layer phase modulated radar absorber," *in 2001 Eleventh International Conference on Antennas and Propagation*, vol. 2, pp. 588-592, 2001.

[4] Y. Q. Li, H. Zhang, Y.-Q. Fu, and N. C. Yuan, "RCS reduction of ridged waveguide slot antenna array using EBG radar absorbing material," *IEEE Antennas Wireless Propag. Lett.*, vol. 7, pp. 473-476, 2008.

[5] H. K. Jang, J. H. Shin, and C. G. Kim, "Low RCS patch array antenna with electromagnetic bandgap using a conducting polymer," *2010 International Conference on Electromagnetics in Advanced Applications*, pp. 140-143, 2010.

[6] D. Feng, H. Zhai, L. Xi, S. Yang, K. Zhang, and D. Yang, "A broadband low-profile circular-polarized antenna on an AMC reflector," *IEEE Antennas Wireless Propag. Lett.*, vol. 16, pp. 2840-2843, 2017.

[7] H. Zhai, K. Zhang, S. Yang, and D. Feng, "A low-profile dual-band dual-polarized antenna with an AMC surface for WLAN applications," *IEEE Antennas Wireless Propag. Lett.*, vol. 16, pp. 2692-2695, 2017.

[8] M. A. Belen, F. Güneş, P. Mahouti, and A. Belen, "UWB gain enhancement of horn antennas using miniaturized frequency selective surface," *ACES Journal*, vol. 33, no. 9, pp. 997-1002, 2018.

[9] Y. Zhao, X. Y. Cao, J. Gao, X. Yao, T. Liu, W. Q. Li, and S. J. Li, "Broadband low-RCS metasurface and its application on antenna," *IEEE Trans. Antennas Propag.*, vol. 64, no. 7, pp. 2954-2962, 2016.

[10] M. Paquay, J. C. Iriarte, and I. Ederra, "Thin AMC structure for radar cross section reduction," *IEEE Trans. Antennas Propag.*, vol. 55, no. 12, pp. 3630-3638, 2007.

[11] Y. C. Song, J. Ding, C. J. Guo, Y. H. Ren, and J. K. Zhang, "Ultra-broadband backscatter radar cross section reduction based on polarization-insensitive metasurface," *IEEE Antennas Wireless Propag. Lett.*, vol. 15, pp. 329-332, 2016.

[12] P. Yao, B. Z. Zhang, and J. P. Duan, "A broadband artificial magnetic conductor reflecting screen and application in microstrip antenna for radar cross-section reduction," *IEEE Antennas Wireless Propag. Lett.*, vol. 17, no. 3, pp. 869-872, 2018.

[13] Y. Zhang, R. Mittra, B. Z. Wang, and N. T. Huang, "AMCs for ultra-thin and broadband RAM design," *Electronics Lett.*, vol. 45, no. 10, pp. 484-485, 2009.

[14] W. G. Chen, C. A. Balanis and C. R. Birtcher, "Checkerboard EBG surfaces for wideband radar cross section reduction," *IEEE Trans. Antennas Propag.*, vol. 63, no. 6, pp. 2636-2645, 2015.

[15] C. Zhang, J. Gao, X. Y. Gao, L. Xu, and J. F. Han, "Low scattering microstrip antenna array using coding artificial magnetic conductor ground," *IEEE Antennas Wireless Propag. Lett.*, vol. 17, no. 5, pp. 869-872, 2018.

[16] Y. Zhang, R. Mittra, and B. Z. Wang, "Novel design for low-RCS screens using a combination of dual-AMC," *2009 IEEE Antennas and Propagation Society International Symposium*, pp. 1-4, 2009.

[17] X. Y. Song, Z. H. Yan, and T. L. Zhang, "Broadband AMC surface for radar cross section reduction," *The 10th International Conference on Microwave and Millimeter Wave Technology*, Chengdu, China, 2018.

[18] Y. Zhao, X. Y. Cao, J. Gao, X. Yao, and X. Liu, "A low-RCS and high-gain slot antenna using broadband metasurface," *IEEE Antennas Wireless Propag. Lett.*, vol. 15, pp. 290-293, 2016.

[19] B. A. Munk, *Frequency Selective Surfaces: Theory and Design*, New York, John Wiley & Sons, 2000.

Xueyan Song was born in Henan Province, China, 1989. She received the B. E. degree in Electronic and Information Engineering from Xidian University, Xi'an, China, in 2012. She received the Ph.D. degree in Electromagnetic Fields and Microwave Technology from Xidian University, Xi'an, China, in 2018.

She joined the School of Electronic Engineering, Xi'an University of Posts and Telecommunications in 2018. Her research interests include artificial magnetic conductors, low RCS antennas, low-profile antennas, frequency selective surfaces, and reflector antennas.

Lei Chen was born in Shaanxi Province, China, 1982. She received the Ph.D. degrees in Electro-magnetic Fields and Microwave Technology from Xidian University, Xi'an, China, in 2010.

She is an Associate Professor at Xidian University. Her research interests include retrodirective array, reflectarray and smart antenna.

Zehong Yan was born in Hubei Province, China, 1964. He received the B.E. degree in Antenna and Microwave from Xidian University, Xi'an, China, in 1984. He received the Ph.D. degree in Electromagnetic Fields and Microwave Technology from Northwestern Polytechnical University, Xi'an, China, in 1996.

He joined the School of Electronic Engineering, Xidian University in 1987 and was promoted to Associate Professor and Professor in 1996 and 2000, respectively, where he is currently a doctoral supervisor with the School of Electronic Engineering. His research interests include communication antennas, satellite tracking antennas, and microwave devices.

Yanyan Li was born in Shanxi Province, China, 1988. She received the B.E. degree in Electronic Information Science and Technology from Xinzhou Teachers University, Xinzhou, China, in 2012. She received the Ph.D. degree in Electromagnetic Fields and Microwave Technology from Xidian University, Xi'an, China, in 2017.

Her research interests include computational electromagnetics, Radar target characteristics and phased array antennas.